SONO-PHOTO-DEGRADATION OF CARBAMAZEPINE IN A THIN FALLING FILM REACTOR: OPERATION COSTS IN PILOT PLANT

A.J. Expósito[1], D.A.Patterson[2], J.M Monteagudo[1], A. Durán*[1]

[1]Department of Chemical Engineering. ETSII. University of Castilla-La Mancha. Avda. Camilo José Cela 3. 13071. Ciudad Real (Spain). Fax: 34 926295361. Phone: 34 926295300, ext: 3814. email: antonio.duran@uclm.es

[2] Department of Chemical Engineering and Centre for Sustainable Chemical Technologies, University of Bath, Bath, United Kingdom, BA2 7AY. email: d.patterson@bath.ac.uk

ABSTRACT

The photo-Fenton degradation of carbamazepine (CBZ) assisted with ultrasound radiation (US/UV/H_2O_2/Fe) was tested in a lab thin film reactor allowing high TOC removals (89% in 35 minutes). The synergism between the UV process and the sonolytic one was quantified as 55.2%.

To test the applicability of this reactor for industrial purposes, the sono-photo-degradation of CBZ was also tested in a thin film pilot plant reactor and compared with a 28 L UV-C conventional pilot plant and with a solar Collector Parabolic Compound (CPC). At a pilot plant scale, a US/UV/H_2O_2/Fe process reaching 60% of mineralization would cost 2.1 and 3.8 €/m^3 for the conventional and thin film plant respectively. The use of ultrasound (US) produces an extra generation of hydroxyl radicals, thus increasing the mineralization rate.

In the solar process, electric consumption accounts for a maximum of 33% of total costs. Thus, for a TOC removal of 80%, the cost of this treatment is about 1.36 €/m^3. However, the efficiency of the solar installation decreases in cloudy days and can not be used during night, so that a limited flow rate can be treated.

Keywords: CPC, economics, pilot plant; radicals; ultrasound; UV

1. INTRODUCTION

Process intensification is about providing a chemical process with the precise environment required which results in better products, and processes which are safer, cleaner, smaller and cheaper [1]. Some features include moving from batch to continuous processing, using new emerging technologies (such as ultrasound) and use of intensive reactor technologies with high mixing and heat transfer rates in place of conventional stirred tanks [2, 3].

Regarding the first feature, homogeneous advanced oxidation processes (AOPs) have been largely used to degrade refractory organic pollutants present in water [4-7]. Sonophotocatalysis (consisting of a combination of ultrasonic sound waves, ultraviolet radiation and a catalyst) has recently emerged as an alternative water treatment method [8-10] due to several advantages: lower doses of catalysts and reagents, no need for low turbidity, etc. However, the use of high-frequency ultrasound demands high amounts of energy, so that an economical study in needed to quantify its applicability in each reactor type.

A previous research [11] showed the important contribution of •OH radicals during degradation of carbamazepine under the US-UV-H_2O_2-Fe system. Under optimum conditions, mineralization reached 93% in 35 minutes under batch conditions. The authors also performed a study of the flow pattern inside the reactor, showing that improvement in mineralization rate with US radiation could not be attributed to a positive effect in mixing. Thus, the aim of this research is focussed on i) understanding the effect of US radiation on the formation of hydroxyl radicals to improve

mineralization, ii) to perform mineralization tests at a pilot plant scale and iii) to analyze the economic viability of the process

Regarding the use of new reactor technologies and in addition to conventional batch reactors, in the last years several new type of reactors have been developed to remove pollutants from water effluents including thin film reactors and collector parabolic compound (CPC). Thin film reactors have a large heat and mass transfer area per unit liquid volume that make them very efficient in industry. They have low contact time, low pressure drop, and easy cleaning. The main inconvenience is that high flow rates induce waves in the falling liquid and the film can be broken. To avoid this trouble, we can use a smaller tube and ensure the perfect verticality of the tube. The flow in the form of a thin film also favors heat exchange, obtaining larger coefficients [12], in case that heating/cooling is necessary in the system. They are also useful when light penetration is not good in a batch reactor. Unfortunately, they are usually less applied for photochemical reactions.

On the other hand, solar photo-Fenton in a compound parabolic collector (CPC) reactor is known to be one of the most environmentally benign and cost-effective systems for wastewater treatment [13-15].

In this work, a simple experimental falling film pilot plant has been constructed, tested and compared with a conventional artificial UV cylindrical reactor. Thus, results in the thin film device have also been compared with those obtained in a solar CPC plant. Carbamazepine (CBZ), a refractory pharmaceutical organic drug not degraded in WWTP processes (removal efficiencies below 10%) has been treated as a model

84 pollutant and a previously optimized photo-Fenton process assisted with ultrasound
85 radiation (US/UV/H_2O_2/Fe) has been used as an intensified AOP. The sonophotolytic
86 degradation of organic compounds has already proved to be effective due to the
87 synergistic effect of the US and UV irradiation [16].
88
89 In order to determine the efficacy of the thin film reactor approach as a process
90 intensification technology for photocatalytic wastewater treatment, an economical
91 analysis has also been made. There are many studies using thin film reactors with TiO_2
92 as a heterogeneous wastewater treatment [17-19]. However, to our knowledge no
93 studies have been made in homogeneous phase comparing technical and economical
94 efficiencies.
95
96 **2. EXPERIMENTAL SET-UP**

97 **2.1. Laboratory scale device**

98 The experimental set-up consists on two glass pipes bundled as a shell-and-tube heat
99 exchanger (inner diameter = 2.75cm; length = 28.3 cm). The CBZ solution flows in the
100 form of a thin film that runs down inside the inner tube where a Heraeus UV immersed
101 lamp TNN 15/32 is located. A pump is used to regulate the flow rate. A wider element
102 in the upper part of the column acts as an overflow system which is responsible for the
103 fluid falling as a film. The optical path lengths in this thin film reactor was obtained to
104 be 1.23 cm. Due to the small dimensions of the thin film, it is ensured that all the
105 radiation coming from the lamp is reaching the wastewater, enhancing the efficiency of
106 the reactor.
107
108

2.2. Pilot plants

2.2.1. UV-Pilot Plant

The UV pilot plant (FLUORACADUS-08/2.2) is shown in Figure 1 and is composed by a 28 L reactor (2240mm x 730mm x 100mm), with four UV-C lamps (280–200 nm) TUV_TL_D_55W_HO_SLV UV-C PHILIPS. The system is able to treat up to 1400 l/h. Temperature (up to 60ºC) is controlled by a digital Fuji PXR4TAY1-1Vcontroller.

2.2.2. CPC Pilot Plant

The CPC consisted of a tank (50 L), a centrifugal recirculation pump, a solar collector unit with an area of 2 m^2 (concentration factor = 1) in an aluminum frame mounted on a fixed south-facing platform tilted 39º in Ciudad Real (Spain) with connecting tubing and valves. The solar unit had 16 borosilicate glass tubes (OD 32 mm) and the total illuminated volume inside the absorber tubes was 16 L. Visible solar radiation (400-600 nm) and UV radiation (200-400 nm) were measured by two Ecosystem model ACADUS radiometers which provided data for the incident UV-A solar power (W m^{-2}) and accumulated solar power (W h).

2.2.3. Thin film pilot plant

This pilot plant has the same configuration that the lab prototype, although now it consists on a two concentric stainless steel tube with higher dimensions (3.8 cm inner diameter; 85 cm height). A 55w submersible lamp (BIO-UV Ultraviolet solutions) was used.

Figure 1

132 **2.3. Experimental runs and analysis**

133 All experiments were carried out at pH =2.7 and 30ºC. A 24 kHz, 200 W direct
134 inmersion horn sonicator (UP200S with an S14 sonotrode, Hielscher) was used to
135 generate ultrasonic sound waves in the sonoreactor in lab devices. The amplitude of the
136 oscillatory system (power output) can be steplessly adjusted between 20% and 100%.
137 The pulse mode factor (cycles) can be continuously varied between 10% and 100%. The
138 set value equals the acoustic irradiation time in seconds, the difference to 1 s is the
139 pause time. Thus, a setting of 1 implies that it is continuously switched on, whereas a
140 setting of 0.6 means a power discharge of 0.6 s and a pause of 0.4 s. Amplitude and
141 pulse length (cycles) were maintained constant at 60% and 1, respectively according to
142 literature [11].

143 On the other hand, a UIP 1000HD230 (Hielscher) with a sound protection box was used
144 in pilot plants installations (see Figure S1 in supplementary material). The main
145 characteristics are: ultrasonic frequency of 20kHz, automatic frequency tuning system,
146 amplitude 25 micron adjustable from 50 to 100%, and dry running protected. The
147 dimensions of the transducer are (LxWxH) 435x110x71mm. The generator uses 230
148 Volts, AC, single phase, 8A, 50-60Hz.A sonotrode (BS2d34) titanium, tip diameter
149 34mm, length 125mm was used.

150 Figure S1

151 More details of reactor configurations and ultrasound power are shown in Table 1.
152 Initial concentration of carbamazepine (CBZ) in deionized water was 78.2 ppm (TOC =
153 55 ppm). The flow rate was 45 L/h in the thin film lab device, 1140 L/h in the
154 conventional and solar pilot plants and 150 L/h in the thin film plant.

155 Table 1

156 CBZ (99%) was obtained from Acros. Analytical grade ferrous sulfate ($FeSO_4 \cdot 7H_2O$),
157 and 30% w/v hydrogen peroxide (H_2O_2) were acquired from Merck. The pH of the
158 wastewater was adjusted with H_2SO_4 and NaOH solutions. Total organic carbon
159 concentration was determined using a TOC analyzer (Shimadzu TOC-5000A).

160

161 Quantification of hydroxyl radicals was carried out using disodium salt of terephthalic
162 acid (NaTA) [20]. NaTA (non-fluorescent) is known as an HO• scavenger; it reacts with
163 HO• to form 2-hydroxyterephthalic acid (HTA, fluorescent). The concentration of HTA
164 was determined by its fluorescence, which yield is proportional to the HO•
165 concentration in the solution in the excess of NaTA.

166 The HTA fluorescence yield was measured with an RF 6000 spectro-fluorophotometer
167 (Shimadzu). The excitation wavelength was set at 315 nm and the fluorescence spectra
168 of the solution were collected in the range of 320 nm - 500 nm. The peak intensity was
169 quantified for each solution at the emission wavelength of 425 nm using a previous
170 calibration.

171 **3. RESULTS AND DISCUSSION**

172 **3.1. Study of UV, US and UV/US processes**

173 Figure 2 shows degradation of CBZ under different processes (UV, US and UV/US) for
174 the lab falling film device. The values of the photolytic constant (k_{UV}) were 0.0264 min^{-1}
175 for CBZ degradation and 0.0019 min^{-1} for mineralization. The values of the sonolytic
176 constant (k_{US}) were 0.0044 min^{-1} for CBZ degradation and 0.002 min^{-1} for
177 mineralization. It was proved that hydrogen peroxide was either not formed under these
178 conditions or it was below detection limits.

179 Figure 2

180 The synergism between the UV process and the sonolytic one can be quantified using
181 the pseudo first order degradation rate constants according to equation (1) [21]:
182
183 $$Synergy\ (\%) = \frac{k_{UV+US} - (k_{UV} + k_{US})}{k_{UV+US}} x\,100 = \frac{0.0688 - (0.0264 + 0.0044)}{0.0688} x100 = 55.23 \quad (1)$$
184
185 **3.2. Determination of optimal operation conditions (US/UV/H_2O_2/Fe)**
186 Figure 3a shows the results for CBZ degradation under different initial H_2O_2
187 concentrations for the system (US/UV/H_2O_2). CBZ was practically completely removed
188 in all the cases, except for at very low hydrogen peroxide concentration (5 ppm).
189 However TOC removal (Figure 3b) reached a maximum of 46% in 35 minutes when
190 using 20 ppm of H_2O_2. Results also showed that the CBZ degradation rate followed a
191 pseudo-first order rate (Figure 3c) with the pseudo-first order kinetic constant increasing
192 with the initial concentration of H_2O_2 from 0.002 to 0.168 min^{-1}, since more radicals are
193 being formed due to photolysis of hydrogen peroxide:
194 $$H_2O_2 + h\nu \rightarrow 2\ \bullet OH \quad (2)$$
195 Figure 3
196 According to literature [11] when the value of the initial concentration of hydrogen
197 peroxide is increased, HO• radicals may recombine or react according to the "well
198 known" scavenger effect, inhibiting the CBZ degradation rate. Thus, in order to
199 improve mineralization results,10 ppm of Fe(II) were added to the system. Then, the
200 mineralization degree increases up to 89% in 35 minutes via generation of extra radicals
201 according to the following reaction:
202 $$Fe\ (II) + H_2O_2 \rightarrow Fe^{(}III) + \bullet OH + OH^- \quad (3)$$

The kinetic mineralization constant, as shown in Figure 3c, increases more than four times, up to 0.075 min^{-1}. Under these selected conditions, the whole study outlined next was developed.

3.3. Study of radicals

Monteagudo at al. [22] studied the sono-photo-Fenton degradation of reactive Blue-4, showing the importance of the different mechanisms. Radical reaction was found to be the main mineralization pathway (93.60%), being the contribution of ultrasonically generated oxidative species to the overall mineralization very low (1.92%). Thus any improvement in the use of US radiation must be related to the radicals involved in mineralization.

The main reactions involved in the sono-photo-Fenton degradation are equations (2) to (8) [23]:

$$H_2O \xrightarrow{)))} \cdot OH_{)))} + \cdot H_{)))} \quad (4)$$

$$CBZ + \cdot OH_{)))} \xrightarrow{k_{US}} \text{Products} + H_2O \quad (5)$$

$$CBZ + h\upsilon \xrightarrow{k_{UV}} \text{Products} \quad (6)$$

$$2 \cdot OH_{)))} (\cdot X) \longrightarrow H_2O_2 \quad (7)$$

$$CBZ + \cdot OH \longrightarrow \text{Products} + H_2O \quad (8)$$

where))) denotes the ultrasonic waves, the subscript))) denotes the products generated by US and (·X) denotes all the possible intermediates leading to forming H_2O_2.

Figure 4 shows a study of the evolution of the concentration of CBZ and hydroxyl radicals during reaction for different processes at lab scale including: H_2O_2, Fenton (H_2O_2/Fe), photo-Fenton (UV/H_2O_2/Fe) and sono-photo-Fenton (US/UV/H_2O_2/Fe).

228 Hydrogen peroxide and Fenton system allow a low degradation of initial CBZ (6% and
229 22% respectively), correlated with the concentration of HO• radicals found in solution
230 (Figure 4b). As expected, the photo-Fenton process improves significantly the CBZ
231 degradation due to generation of extra hydroxyl radicals via reaction (2). Finally, it can
232 be seen that the sono-photo-Fenton process is the fastest degradation process. The
233 amount of hydroxyl radicals is slightly higher at the beginning of reaction, favoring
234 CBZ degradation and later mineralization. This fact confirms that the radical reaction is
235 the main mineralization pathway.

236 Figure 4

237 **3.3. Comparing pilot plant devices: economical study**

238 At an industrial scale, high flowrates of effluents must be treated, so that pilot plant tests
239 are necessary to confirm the above preliminary results. To this end, three pilot plants
240 were selected: a) thin film, b) a 28 L reactor with four UV-C lamps working as two
241 concentric tubes in continuous mode and c) a solar compound parabolic collector (CPC)
242 plant with an area of 2 m^2 in order to reduce costs coming from electricity.

243

244 Figure 5a shows the results for TOC degradation in both the UV classical pilot plant and
245 the thin film one. Reactor configurations are summarized in Table 1. 70 % of TOC is
246 removed in the thin film photo-reactor and 90% in the classical pilot plant after 2.5
247 hours. However, the classical UV plant uses a higher amount of energy, since four
248 lamps are being used. An economical approach is thus needed to evaluate the possible
249 application of a thin film device at an industrial scale.

250 Figure 5

To this end, prices of materials (reagents and catalyst) and electrical consumption of the different devices used for calculation of costs are shown in Table 2, whereas Table 3 summarizes the amount of reagents and catalysts consumed in each processes.

Table 2, Table 3

The whole economic analysis was carried out considering the mineralization process. Figure 5b shows operation costs both for the thin film and the UV classical pilot plant in terms of Euros per cubic meter of treated water. It is confirmed that costs increases when high percentages of TOC removal are needed in both processes, and dramatically increases for removals > 80%. Usually, a complete mineralization is not required and advanced oxidation processes (AOPs) can be designed with the subsequent biological treatment process that treats products from AOPs [24]. Thus, for a 60% of mineralization, costs would raise to 2.1 and 3.8 €/m^3 for the UV-classical and thin film plant respectively. However, electricity costs account for the 70 % (thin film) and 50% (classical device) of total cost (Figure 5c). In order to reduce electricity costs for their possible use in an industrial application, the following new experiments were performed:

a) due to the high power consumption cost of the US probe, new tests were made with the former pilot plants under the photo-Fenton system (UV/H_2O_2/Fe) without US radiation (for the case that operation time is not decisive; otherwise the use of US is mandatory)
b) substitution of artificial UV radiation with solar energy. Thus, a solar CPC pilot plant was used and compared with the previous results. In this case, oxalic acid was added to the system (mole ratio Fe:$(COOH)_2$ =3) to form ferrioxalates and improve degradation rate due to generation of Fe(II) through a well-known

mechanism [8]. Moreover, the use of ferrioxalates implies that a higher portion of the solar spectrum can be used.

When experiments without US are analyzed (Figure 6a), the time needed to reach the same mineralization degree increases, as previously explained due to the reduction in hydroxyl radicals available for mineralization of CBZ. For example, for 70 % of TOC removal, ~5.5 hours are now needed in the thin film photo-reactor (~2.5 hours with US), whereas 95 min are employed in the UV conventional plant (40 min with US). However, although the process in clearly faster with US and in the conventional UV pilot plant, the cost study (Figure 6b) indicates that now the thin film device is competitive compared to the UV conventional plant (please note that the thin film plant has just one 55W lamp, whereas the conventional one uses four of them). Costs around 2 €/m^3 are obtained in both systems for a 50% of TOC removal.

Figure 6

Regarding the solar process, and in order to compare experiments over several days, it is necessary to use a simple equation to normalize the data so that the time used in Figures comes from the following correlation [25]:

$$t_{30W,n} = t_{30W,n-1} + \Delta t_n \frac{UV}{30}\frac{V_i}{V_T};\ \Delta t_n = t_n - t_{n-1};\ t_0 = 0\ \ (n=1) \qquad (9)$$

where t_n is the experimental time for each sample, UV is the average solar ultraviolet radiation ($\lambda < 400$ nm) measured between t_{n-1} and t_n, and t_{30W} is a normalized illumination time that refers to a constant solar power of 30 Wm^{-2} (typical solar UV radiation on a perfectly sunny day around noon). V_T is the total reactor volume and V_i is the total irradiated volume.

299 The solar process is definitively faster during the first 30 minutes as shown in Figure 6a
300 (70% of mineralization in 16 min). Then mineralization is slower because most of
301 hydrogen peroxide in solution has been consumed. Also costs per unit of volume of
302 water treated are considerably lower as seen in Figure 6b (around 1.3 €/m^3 up to 80 %
303 of mineralization). This is due to the low electric consumption that in the CPC pilot
304 plant accounts for 2-33% of total costs, whereas it varies from 60-90% in the thin film
305 device and from 5-61% in the conventional UV plant depending on the desired
306 mineralization degree (Figure 7).

307 Figure 7

308 However, the efficiency of the solar installation decreases in cloudy days and it cannot
309 be used during the night, so that a limited flow rate of effluent can be treated, unless a
310 mixed installation including artificial UV lamps is used.

311

312 Finally, Figure 8 shows that operation cost (€/g TOC removed) gradually decreases as
313 TOC removal is higher for the three pilot plants studied. In this way we fully benefit
314 from the reagents that are added in one go at the beginning of the process.

315 Figure 8

316 Note that this study intends to be an initial guide only. A bigger thin film plant should
317 be tested to confirm these preliminary results. For this reason, only operation costs have
318 been estimated; the investment cost, the salvage value, the estimated useful life,
319 depreciation expense for year and maintenance are not considered here.

320

321 Obviously, the concentration of pollutants reaching a Waste Water Treatment Plant
322 (WTTP) would be lower than the one treated here and the oxidation processes could be
323 used as a primary step before the biological process, so that very high mineralization

degrees would not be required. The operational costs obtained here could then be decreased at an industrial scale and when taking into account all these considerations. Also, the use of photovoltaic panels could decrease costs when using CPC devices [26].

4. CONCLUSIONS

- An important synergistic effect between sonolysis and UV irradiation of 55.2% was quantified using the first order rate constants for carbamazepine degradation.
- At a pilot plant scale, a US/UV/H_2O_2/Fe process reaching 60% of mineralization would cost 2.1 and 3.8 €/m^3 for the conventional and thin film plant respectively. The use of US makes the process faster, due to extra hydroxyl radicals generated, but more expensive.
- At a pilot plant scale under a UV/H_2O_2/Fe process, both the thin film device and the UV conventional plant are comparable in terms of operational costs (~ 2 €/m^3 for a 50% of TOC).
- The solar process is faster and cheaper (around 1.3 €/m^3 up to 80 % of mineralization), since electric consumption accounts for a maximum of 33% of total costs. However, the efficiency of the solar installation decreases in cloudy days and cannot be used during the night, so that a mixed installation including artificial UV lamps must be used if high flowrates have to be treated.

5. ACKNOWLEDGEMENTS

Financial support from MINECO (CTM2013-44317-R) is gratefully acknowledged.

5. REFERENCES

[1] (http://profmaster.blogspot.com.es/2011/03/process-intensification-1.html).

[2] I.A. Boiarkina, S. Norris, D.A. Patterson, The Case for the Photocatalytic Spinning Disc Reactor as a Process Intensification Technology: Comparison to an Annular Reactor for the Degradation of Methylene Blue, Chem. Eng. J. 225 (2013) 752–765

[3] I.A. Boiarkina, S. Pedron, D.A. Patterson, An Experimental and Modelling Investigation of the Effect of the Flow Regime on the Photocatalytic Degradation of Methylene Blue on a Thin Film Coated Ultraviolet Irradiated Spinning Disc Reactor. Appl. Catal. B: Environ. 110, (2011) 14-24.

[4] M.A. Oturan, J.J. Aaron, Advanced Oxidation Processes in Water/Wastewater Treatment: Principles and Applications. A Review, Crit. Rev. Env. Sci. Tech., 44 (2014) 2577-2641

[5] L. G. Covinich, D. I. Bengoechea, R. J. Fenoglio, M.C. Area. Advanced Oxidation Processes for Wastewater Treatment in the Pulp and Paper Industry: A Review, Am. J. Environ. Eng. 4 (2014) 56-70.

[6] I. Oller, S. Malato, J.A. Sánchez-Pérez, Combination of Advanced Oxidation Processes and biological treatments for wastewater decontamination-A review. Sci. Total Environ. 409(20) (2011) 4141-4166.

[7] D. Hermosilla, N. Merayo, A. Gascó, A. Blanco, The application of advanced oxidation technologies to the treatment of effluents from the pulp and paper industry: a review. Environ. Sci. Poll. Res Int. 22 (2015) 168-191.

[8] W.H. Song, T. Teshiba, K. Rein, K.E. O'Shea, Ultrasonically induced degradation and detoxification of microcystin-LR (cyanobacterial toxin), Environ. Sci. Technol. 39 (2005) 6300-6305.

371 [9] C.G. Joseph, G. Li Puma, A. Bono, Y.H. Taufiq-Yap, D. Krishnaiah, Operating
372 parameters and synergistic effects of combining ultrasound and ultraviolet irradiation in
373 the degradation of 2,4,6-trichlorophenol, Desalination 276 (2011) 303-309.
374 [10] A. Durán, J.M. Monteagudo, I. Sanmartín, P. Gómez, Homogeneous
375 sonophotolysis of food processing industry wastewater: Study of synergistic effects,
376 mineralization and toxicity removal, Ultrason. Sonochem. 20 (2013) 785-791.
377 [11] A. Durán, J.M. Monteagudo, A.J. Expósito, V. Monsalve, Modelling the
378 sonophoto-degradation/mineralization of in press carbamazepine in aqueous solution,
379 Chem. Eng. J. (2015) 284, 503-512.
380 [12] C. Moraga, M. Carmona, A. Durán Assembly of a Thin-Falling-Film Exchanger
381 for Laboratory Demonstrations: Calculation of the Individual Heat-Transfer Coefficient,
382 Chem. Educator, 6 (2001) 15–20.
383 [13] M. Jiménez, I. Oller, M.I. Maldonado, S. Malato, A. Hernández-Ramírez, A.
384 Zapata, J.M. Peralta-Hernández, Solar photo-Fenton degradation of herbicides partially
385 dissolved in water, Catal. Today 161 (2011) 214-220.
386 [14] A.G. Trovó, T.F.S. Silva, O. Gomes, A.E.H. Machado, W.B. Neto, P.S. Muller, D.
387 Daniel, Degradation of caffeine by photo-Fenton process: Optimization of treatment
388 conditions using experimental design, Chemosphere 90 (2) (2013) 170-175
389 [15] T. Velegraki, D. Mantzavinos, Solar photo-Fenton treatment of winery effluents in
390 a pilot photocatalytic reactor, Catal. Today 240 (2015) 153-159
391 [16] L.J. Xu, W. Chu, N. Graham, Sonophotolytic degradation of dimethyl phthalate
392 without catalyst: Analysis of the synergistic effect and modeling, Water Res., 47 (2013)
393 1996.

394 [17] O.M. Alfano, D. Bahnemann, A.E. Cassano, R. Dillert, R. Goslich, Photocatalysis
395 in water environments using artificial and solar light, Catalysis Today 58 (2000) 199–
396 230.
397 [18] G. Li Puma, P. L. Yueb, Modelling and design of thin-film slurry photocatalytic
398 reactors for water purification, Chem. Eng. Sci. 58 (2003) 2269-2281.
399 [19] G. Li Puma, Modeling of thin-film slurry photocatalytic reactors affected by
400 radiation scattering, Environ. Sci. & Technol. 37 (2013) 5783-5791.
401 [20] M. Saran, K.H. Summer, Assaying for hydroxyl radicals: hydroxylated
402 terephthalate is a superior fluorescene marker than hydroxylated benzoate. Free Rad
403 Res. 31(5) (1999) 429-436.
404 [21] C.G. Joseph, G. Li Puma, A. Bono, Y.H. Taufiq-Yap, D. Krishnaiah, Operating
405 parameters and synergistic effects of combining ultrasound and ultraviolet irradiation in
406 the degradation of 2,4,6-trichlorophenol, Desalination 276 (2011) 303-309.
407 [22] J. M. Monteagudo, A. Durán, I. Sanmartín, S. García. Ultrasound-assisted
408 homogeneous photocatalytic degradation of RB4 in aqueous solution. Appl. Catal. B:
409 Environ., 152-163 (20141) 59-67.
410 [23] L.J. Xu, W. Chu, N. Graham, Sonophotolytic degradation of dimethyl phthalate
411 without catalyst: Analysis of the synergistic effect and modeling, Wat. Res., 47 (2013)
412 1996-2004.
413 [24] K. J. Howe, D.W. Hand, J.C. Crittenden, R. Rhodes-Trussell, G. Tchobanoglous
414 Principles of Water Treatment. (2012). Ed. Wiley.
415 [25] N. Klamerth, L. Rizzo, S. Malato, M.I. Maldonado, A. Agüera, A.R. Fernández-
416 Alba, Degradation of fifteen emerging contaminants at □g L-1 initial concentrations by
417 mild solar photo-Fenton in MWTP effluents, Wat. Res. 44 (2010) 545-554.

[26] A. Durán, J.M. Monteagudo, I. Sanmartín, A. Valverde, Solar photodegradation of antipyrine in a synthetic WWTP effluent in a semi-industrial installation, Sol. Ener. Mat. Sol. C., 125 (2014) 215-222.

443 **FIGURE CAPTIONS**

444 **Figure 1.** Pilot plant devices. a) Thin film (units in mm); b) conventional UV reactor; c)
445 Solar CPC .

446 **Figure 2.** Synergic effect of UV and US on CBZ degradation at the lab thin film device.
447 a) Degradation of CBZ. b) Calculation of kinetic constants

448 **Figure 3.** Experiments under US/UV/H_2O_2 and US/UV/H_2O_2/Fe systems. a) Evolution
449 of CBZ degradtion; b) evolution of TOC degradation; c) Fitting of pseudo first-order
450 mineralization constants

451 **Figure 4.** Formation of hydroxyl radicals under different processes. (Conditions: [H_2O_2]
452 = 20 ppm; [Fe(II)] = 10 ppm). a) CBZ degradation; b) Evolution of hydroxyl radicals.

453 **Figure 5.** Comparison of different pilot plants for the US/UV/H_2O_2/Fe process. a) TOC
454 decrease; b) Operation costs per m^3 of treated water vs mineralization degree; c) Main
455 component of costs in each process for a 60 % of mineralization.

456 **Figure 6.** Comparison of different pilot plants for the UV/H_2O_2/Fe process. a) TOC
457 decrease; b) Operation costs per m^3 of treated water vs mineralization degree.

458 **Figure 7.** Operational costs (reagents and electricity) vs TOC removal. a) Thin film; b)
459 Conventional UV pilot plant; c) Solar CPC. (Process: UV/H_2O_2/Fe)

460 **Figure 8.** Operation costs per g of TOC removed for each process as a function
461 mineralization degree for pilot plants. (Process: UV/H_2O_2/Fe)

462

463

464

Table 1. Reactor configurations and mineralization results.

REACTOR	Volume (l)	Nominal UV power (W)	Measured UV power (W)	US (W)	Mineralization degree (%) and time needed (min)	
	Laboratory device					
Thin film	0.43	15	23.2	168.5	90.0	35
	Pilot plant devices with US					
Conventional UV Pilot plant	33	55×4	208.4	387.8	87.0	120
Thin film		55	51.8		71.6	150
	Pilot plant devices without US					
Solar CPC	33	--	--	--	80.6	25.9
Conventional UV Pilot plant		55×4	208.4		76.7	120
Thin film		55	51.8		77.2	360

Table 2. Electric power and prices of electricity and reagents

ELECTRIC POWER	
*UV Pilot plant**	
Lamps	0.208 kW
Pump	0.050 kW
pH-meter	0.006 kW
Sonotrode	0.387 kW
*Solar CPC pilot plant**	
Pump	0.050 kW
pH-meter	0.006 kW
*Thin Film pilot plant**	
Pump	0.050 kW
Lamp	0.0518 kW
pH-meter	0.006 kW
Sonotrode	0.387 kW
ENERGY PRICE (industrial rate) [UNESA, 2011]	
0,09122 €/kWh	
REAGENTS PRICES	
Hydrogen peroxide	0,445 €/L
Iron (II) sulphate	0,75 €/kg
Oxalic acid	2,6 €/kg
Sulphuric acid	0,183 €/L

** consumption of some components like signal transformers has not been estimated due to its low value*

Table 3. Amount of reagents consumed in each pilot plant

	Conventional UV	Solar CPC	Thin film
Volume of water treated (L)	33	33	33
H_2O_2 (L)	0.075	0.075	0.075
$FeSO_4$ (II) (g)	1.64	1.64	1.64
$H_2C_2O_4$ (g)	-	-	1.38
H_2SO_4 (L)	0.013	0.012	0.011

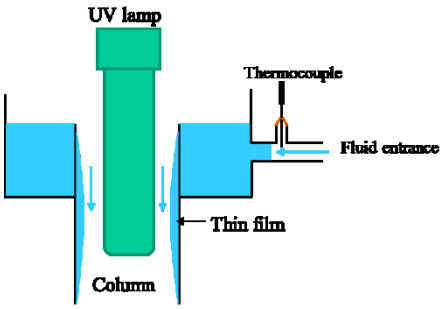
UV lamp
Thermocouple
Fluid entrance
Thin film
Column

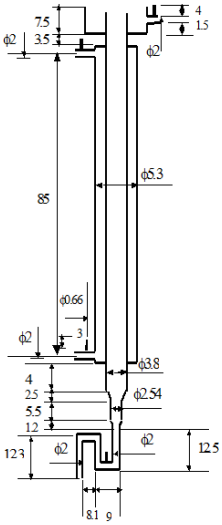
7.5
3.5
ϕ2
4
1.5
ϕ2
ϕ5.3
85
ϕ0.66
ϕ2
3
ϕ3.8
4
2.5
5.5
1.2
ϕ2.54
ϕ2
12.5
12.3
ϕ2
8.1
9

a)


hielscher
Ultrasound Technology

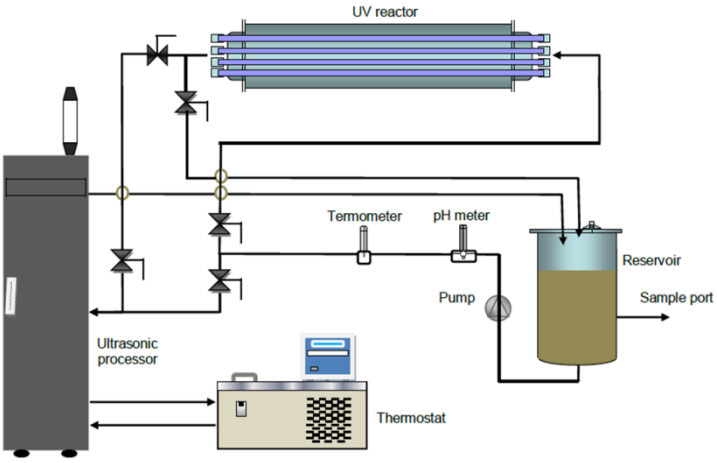
UV reactor
Termometer
pH meter
Reservoir
Pump
Sample port
Ultrasonic processor
Thermostat

b)


radiometers

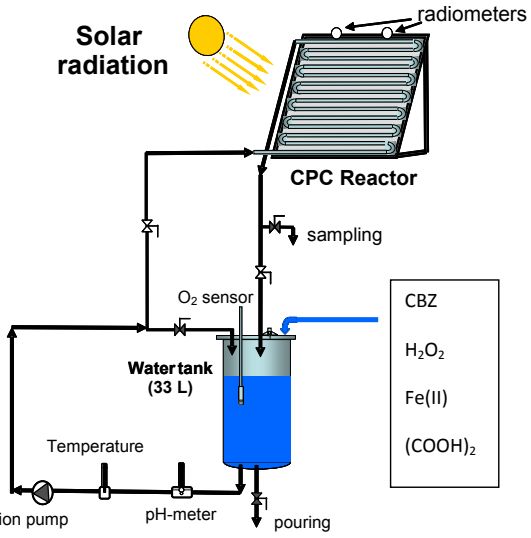
radiometers
Solar radiation
CPC Reactor
sampling
O2 sensor
CBZ
H2O2
Fe(II)
(COOH)2
Water tank (33 L)
Temperature
Recirculation pump
pH-meter
pouring

c)

FIGURE 1

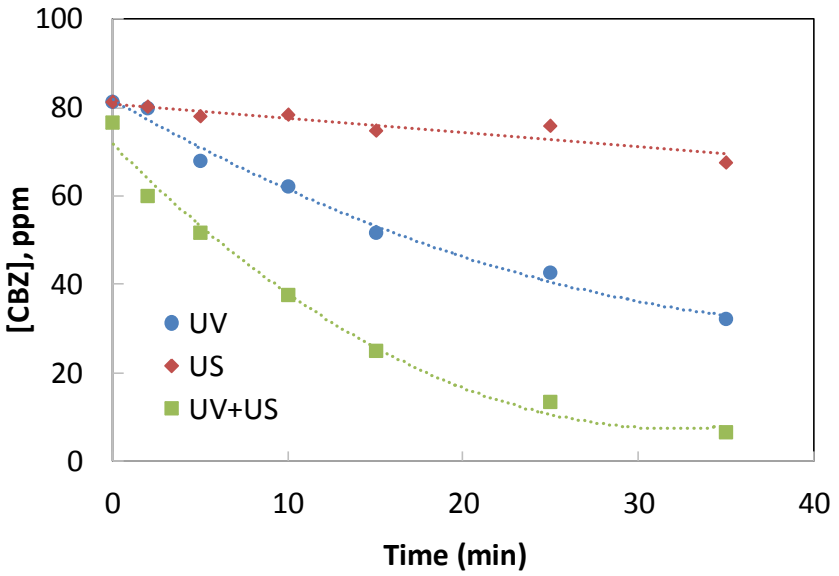
100
80
60
40
20
0
[CBZ], ppm
UV
US
UV+US
0
10
20
30
40
Time (min)

a)

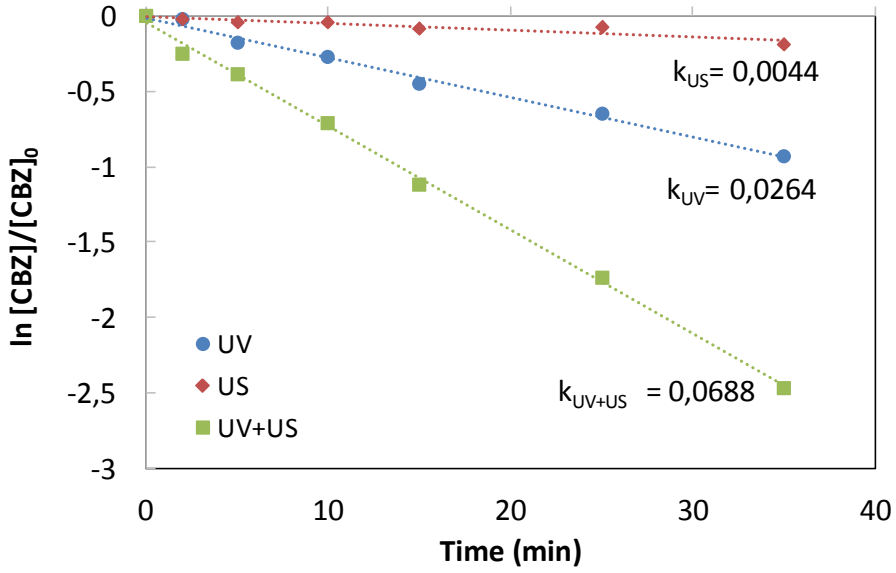
0
-0,5
-1
-1,5
-2
-2,5
-3
ln [CBZ]/[CBZ]0
kUS= 0,0044
kUV= 0,0264
kUV+US = 0,0688
UV
US
UV+US
0
10
20
30
40
Time (min)

b)

FIGURE 2

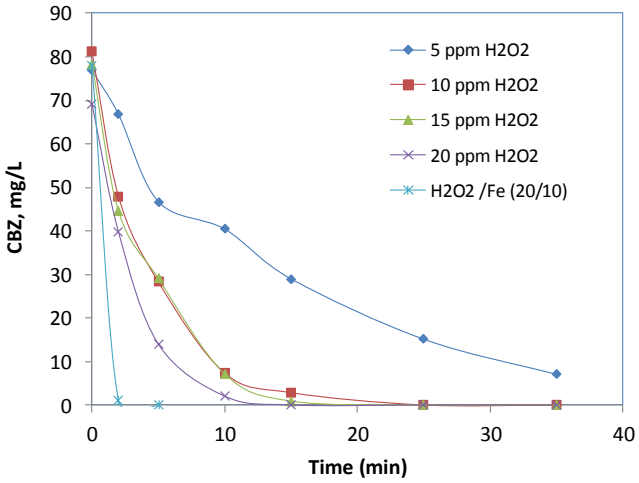
CBZ, mg/L
Time (min)
5 ppm H2O2
10 ppm H2O2
15 ppm H2O2
20 ppm H2O2
H2O2 /Fe (20/10)

a)

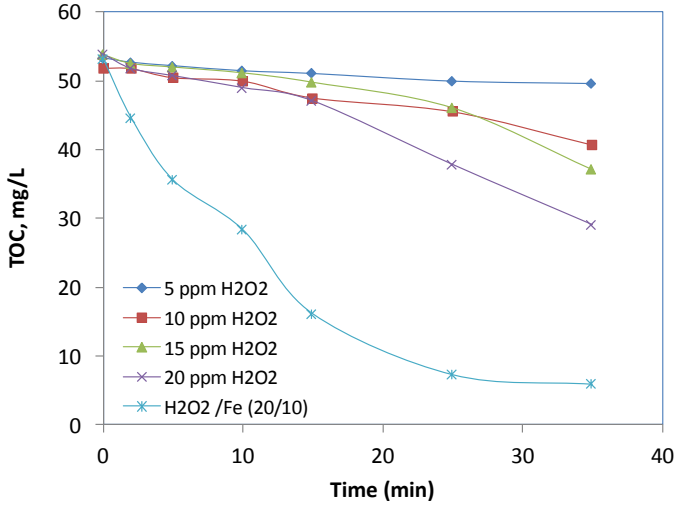
TOC, mg/L
Time (min)
5 ppm H2O2
10 ppm H2O2
15 ppm H2O2
20 ppm H2O2
H2O2 /Fe (20/10)

b)

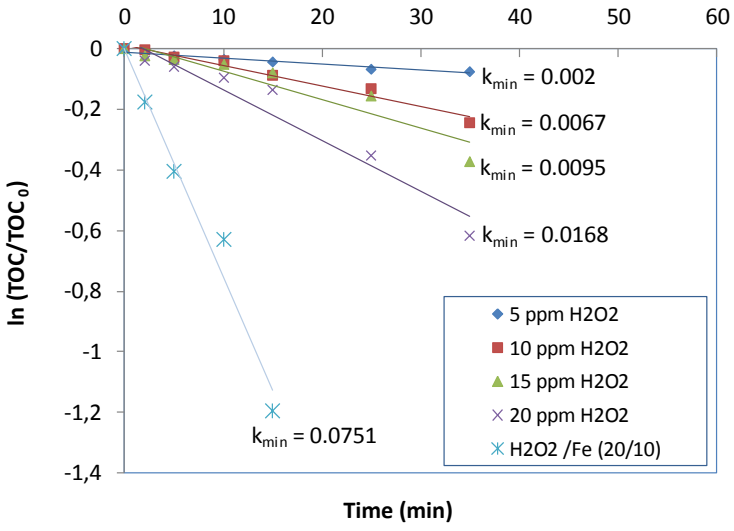
ln (TOC/TOC0)
Time (min)
kmin = 0.002
kmin = 0.0067
kmin = 0.0095
kmin = 0.0168
kmin = 0.0751
5 ppm H2O2
10 ppm H2O2
15 ppm H2O2
20 ppm H2O2
H2O2 /Fe (20/10)

c)

FIGURE 3

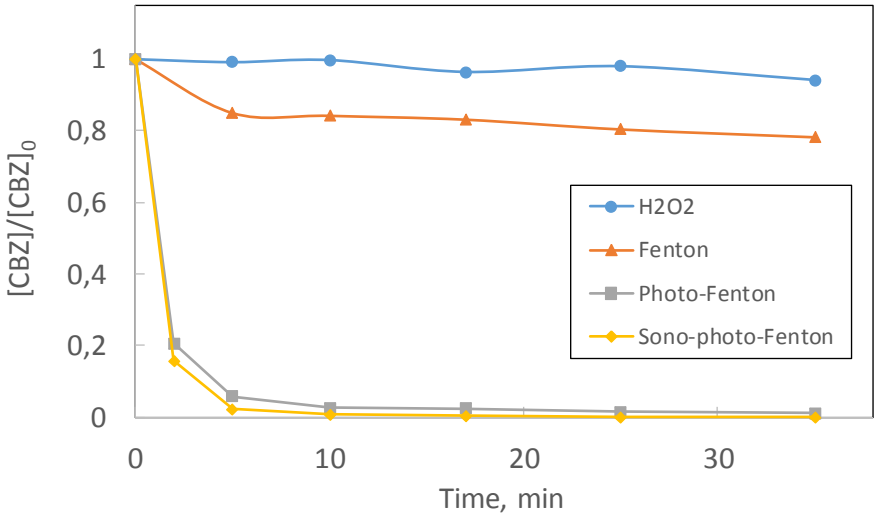
1
0,8
0,6
0,4
0,2
0
[CBZ]/[CBZ]0
0
10
20
30
Time, min
H2O2
Fenton
Photo-Fenton
Sono-photo-Fenton

a)

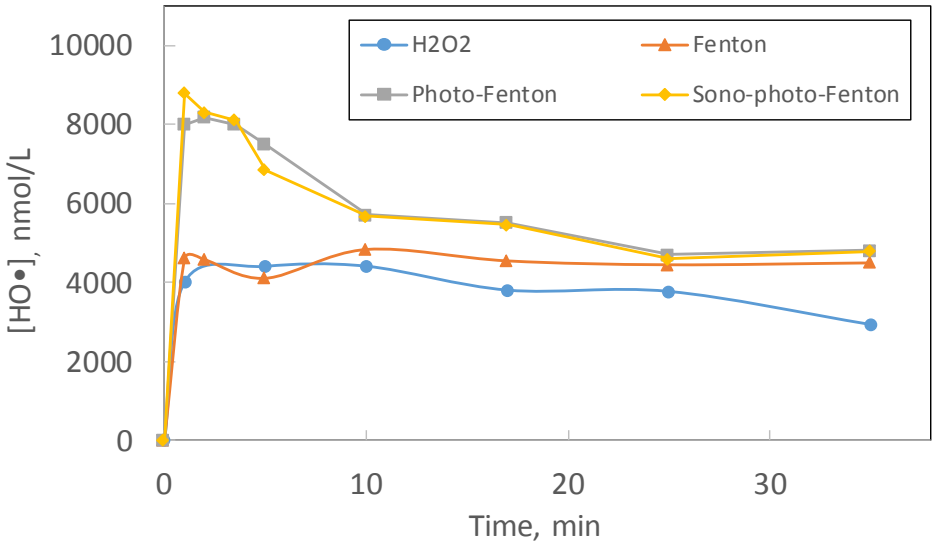
10000
8000
6000
4000
2000
0
[HO•], nmol/L
0
10
20
30
Time, min
H2O2
Fenton
Photo-Fenton
Sono-photo-Fenton

b)

FIGURE 4

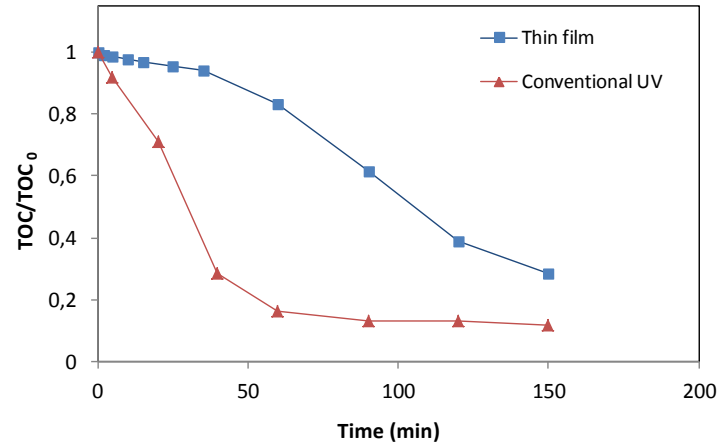
Thin film
Conventional UV
TOC/TOC0
Time (min)
0
0,2
0,4
0,6
0,8
1
0
50
100
150
200

a)

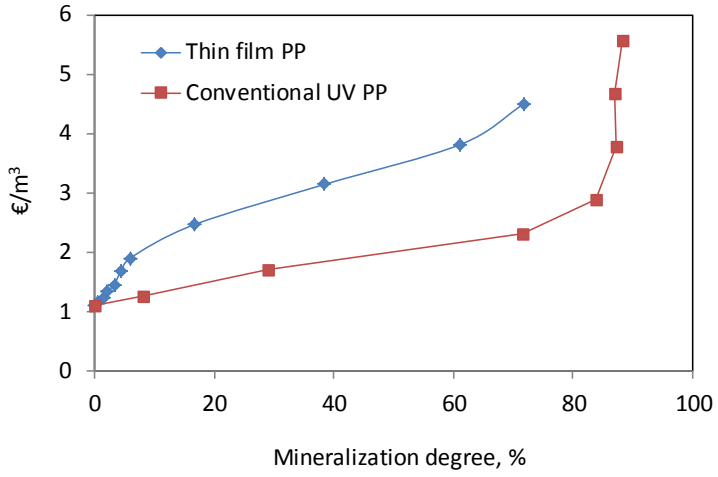
Thin film PP
Conventional UV PP
€/m3
Mineralization degree, %
0
1
2
3
4
5
6
0
20
40
60
80
100

b)

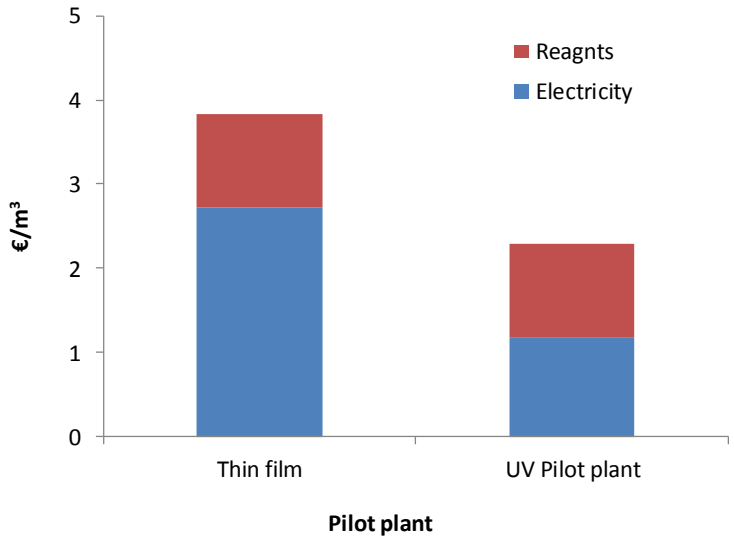
Reagnts
Electricity
€/m3
Thin film
UV Pilot plant
Pilot plant
0
1
2
3
4
5

c)

FIGURE 5

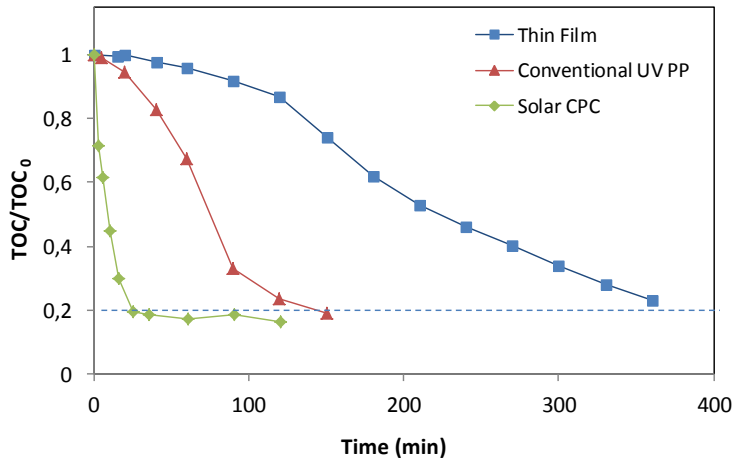
Thin Film
Conventional UV PP
Solar CPC
TOC/TOC0
1
0,8
0,6
0,4
0,2
0
0
100
200
300
400
Time (min)

a)

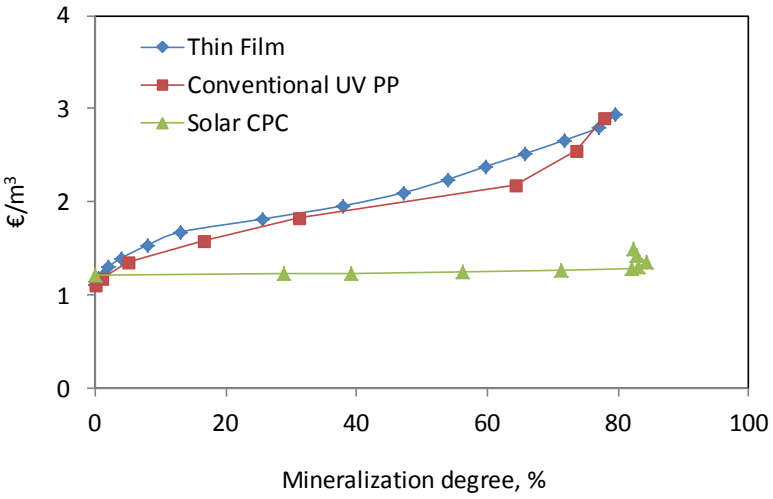
Thin Film
Conventional UV PP
Solar CPC
€/m3
4
3
2
1
0
0
20
40
60
80
100
Mineralization degree, %

b)

FIGURE 6

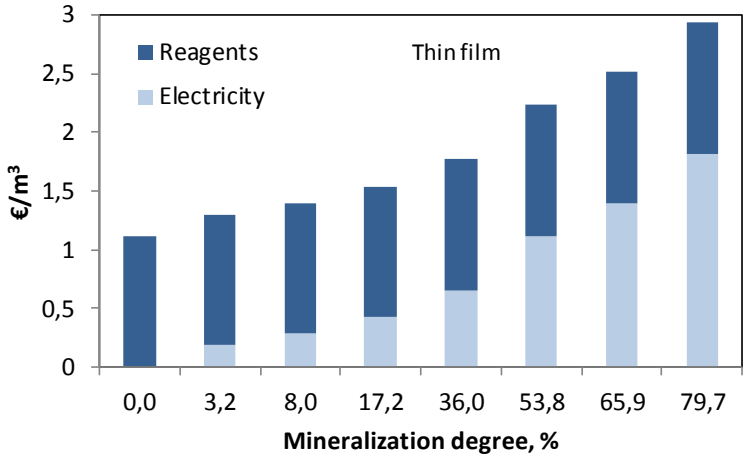
Reagents
Electricity
Thin film
€/m³
3
2,5
2
1,5
1
0,5
0
0,0
3,2
8,0
17,2
36,0
53,8
65,9
79,7
Mineralization degree, %

a)

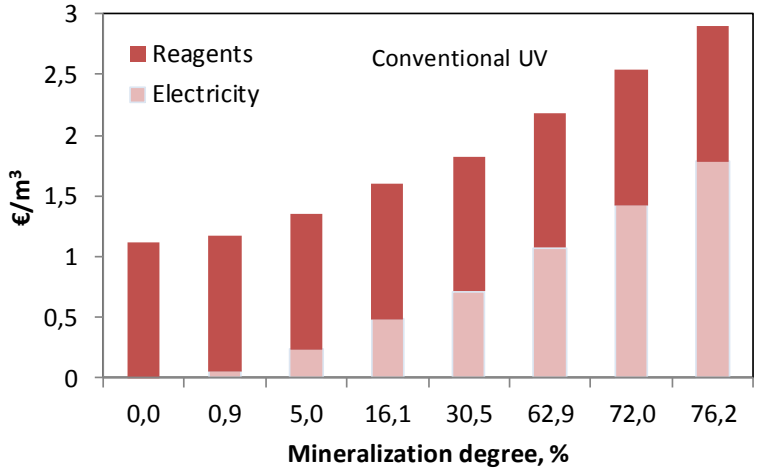
Reagents
Electricity
Conventional UV
€/m³
3
2,5
2
1,5
1
0,5
0
0,0
0,9
5,0
16,1
30,5
62,9
72,0
76,2
Mineralization degree, %

b)

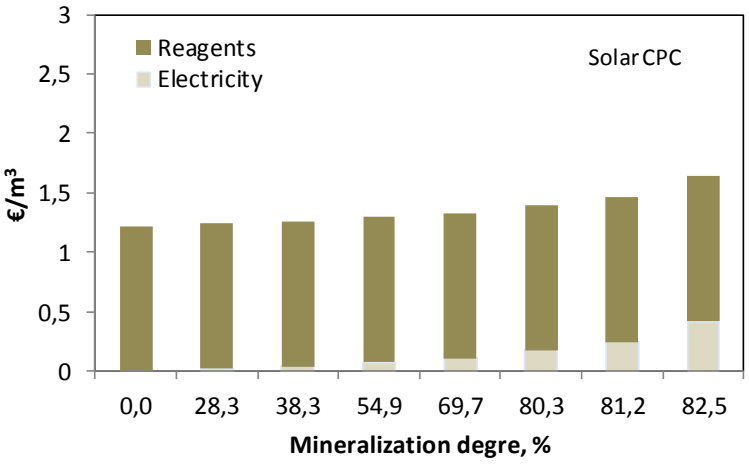
Reagents
Electricity
Solar CPC
€/m³
3
2,5
2
1,5
1
0,5
0
0,0
28,3
38,3
54,9
69,7
80,3
81,2
82,5
Mineralization degre, %

c)

FIGURE 7

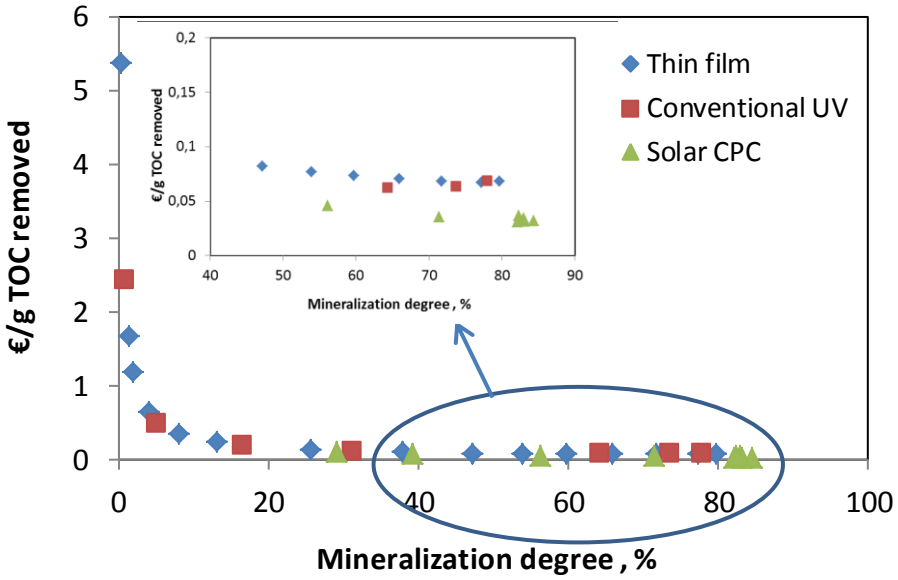
€/g TOC removed
Mineralization degree , %
Thin film
Conventional UV
Solar CPC
0
1
2
3
4
5
6
0
20
40
60
80
100
0,2
0,15
0,1
0,05
0
40
50
60
70
80
90
€/g TOC removed
Mineralization degree , %

FIGURE 8